Received: 6 December 2021 | Accepted: 16 June 2022

DOI: 10.1002/bab.2423

ORIGINAL ARTICLE

WILEY

Structural and functional analyses of GH51 alpha-L-arabinofuranosidase of *Geobacillus vulcani* GS90 reveal crucial residues for catalytic activity and thermostability

Yusuf Sürmeli[1,2] | **Gülşah Şanlı-Mohamed**[1,3]

[1]Department of Biotechnology and Bioengineering, İzmir Institute of Technology, İzmir, Turkey

[2]Department of Agricultural Biotechnology, Tekirdağ Namık Kemal University, Tekirdağ, Turkey

[3]Department of Chemistry, İzmir Institute of Technology, İzmir, Turkey

Correspondence
Gülşah Şanlı-Mohamed, Izmir Institute of Technology, Science Faculty, Department of Chemistry, Urla, Izmir, 35430, Turkey.
Email: gulsahsanli@iyte.edu.tr, gulsahsanli@hotmail.com

Abstract

Alpha-L-arabinofuranosidase (Abf) is of big interest in various industrial areas. Directed evolution is a powerful strategy to identify significant residues underlying Abf properties. Here, six active variants from GH51 Abf of *Geobacillus vulcani* GS90 (*Gv*Abf) by directed evolution were overproduced, extracted, and analyzed at biochemical and structural levels. According to the activity and thermostability results, the most-active and the least-active variants were found as *Gv*Abf51 and *Gv*Abf52, respectively. *Gv*Abf63 variant was more active than parent *Gv*Abf by 20% and less active than *Gv*Abf51. Also, the highest thermostability belonged to *Gv*Abf52 with 80% residual activity after 1 h. Comparative sequence and structure analyses revealed that *Gv*Abf51 possessed L307S displacement. Thus, this study suggested that L307 residue may be critical for *Gv*Abf activity. *Gv*Abf63 had H30D, Q90H, and L307S displacements, and H30 was covalently bound to E29 catalytic residue. Thus, H30D may decrease the positive effect of L307S on *Gv*Abf63 activity, preventing E29 action. Besides, *Gv*Abf52 possessed S215N, L307S, H473P, and G476C substitutions and S215 was close to E175 (acid–base residue). S215N may partially disrupt E175 action. Overall effect of all substitutions in *Gv*Abf52 may result in the formation of the C–C bond between C171 and C213 by becoming closer to each other.

KEYWORDS

directed evolution, error-prone PCR (epPCR), *Geobacillus vulcani*, GH51 family, α-L-arabinofuranosidase

1 | INTRODUCTION

Hemicellulose, the most second abundant native polysaccharide, is one of the major units of lignocellulose from the plant cell wall.[1] It is mainly composed of xylan, which comprises a β-1,3-linked L-arabinose and α-1,2-linked

Abbreviations: ABF, Alpha-L-arabinofuranosidase; GVABF, Abf of Geobacillus vulcani GS90; GH, Glycoside hydrolase; CAZy, Carbohydrate Active Enzyme; pNPA, pNP-α-L-arabinofuranoside; IPTG, isopropyl β-d-1-thiogalactopyranoside; LB broth, Luria-Bertani broth; E. coli, Escherichia coli.

D-glucopyranose with a branch from the xylan backbone consisting of β-1,4-linked xylopyranose.[2,3] Full degradation of xylan is performed by its cooperation with xylanolytic enzymes, including alpha-L-arabinofuranosidases. Alpha-L-arabinofuranosidase (Abf) (E.C.3.2.1.55) hydrolyzes the α-L-arabinosides (polysaccharides carrying arabinose such as arabinoxylan and 1-arabinan) at the terminal and non-reducing α-1,2-, α-1,3-, and/or α-1,5-l-arabinofuranoside constituents.[4] Abf is classified according to the homology of amino acid sequences and the three-dimensional structure of catalytic domains. They fall into nine glycoside hydrolase (GH) families (GH2, GH3, GH5, GH10, GH39, GH43, GH51, GH54, and GH62) as shown in the Carbohydrate Active Enzymes (CAZy) database[5] (http://www.cazy.org/).

Currently, hemicellulases including Abf are of great interest in diverse biotechnological areas, such as the synthesis of pharmaceutics, food processing (wine, bread quality, fruit juice clarification, etc.), the pre-bleaching process of paper pulp, feed additives in farm animals, and production of fermentable sugars for bioethanol generation.[6] Abf has a promising contribution by its synergy with the other hemicellulases in the agro-industrial processes[7,8] and this ensures the productive breakdown of hemicellulose.[9] Thus, Abf, a significant accessory enzyme, is evaluated to be necessary for the increase of cooperative action of hemicellulases.

Abf enzymes are found in various sources such as bacteria, fungi, and plants.[10–12] Thermophilic Abf enzymes are generally preferred in most of the biotechnological fields because industrial operations are generally applied at elevated temperatures.[13–15] So far, GH51 Abf action has been detected in some groups of thermophilic microorganisms including *Geobacillus* genera.[14,16–20] Recently, we have heterologously expressed and biochemically characterized Abf of thermophilic *Geobacillus vulcani* GS90 (*Gv*Abf).[18]

Directed enzyme evolution, which mimics the Darwinian evolution at a lab scale, is a powerful strategy to enhance protein stability and action in different conditions. It relies on random mutagenesis for the enhancement of variations in a gene using successive rounds of screening and selection.[21–23] In literature, this strategy has been successfully implemented for the improvement of various features of Abf enzymes such as catalytic performance, thermostability, and pH stability. These works have elucidated some key residues underlying the improved characteristics of the Abf enzymes.[24–26] Regarding this, Sürmeli and colleagues (2019) have shown that L307 may be a significant residue for the *Gv*Abf activity because L307S amino acid substitution increases the specific activity of this enzyme by approximately 2.5-fold.[24] Also, another study has reported the enhancement of production of xylooligosaccharides (XOs) by 38 variants of GH51 Abf improved via directed evolution. The structure–function analysis of this study has shown that the amino acid substitutions of L352M, M272L, Q316L, I345L, V173D, N344I, and N344Y in five mutants are located at the catalytic domain of GH51 Abf, thereby enhancing XOs production.[25] In addition, Giacobbe et al. (2014) have developed catalytic performance of GH51 Abf and they revealed amino acid substitutions of F435Y and Y446F, which is critical for this property.[26] Thus, directed enzyme evolution appears to be an effective strategy to identify important residues underlying Abf enzyme characteristics.

In the present work, active recombinant *Gv*Abf variants obtained from *G. vulcani* GS90 (*Gv*Abf) by directed evolution were overproduced and extracted by ultrasonication. Activity and thermal stability assays were performed on the soluble protein extracts including each variant. The gene variants were sequenced by the Sanger method and determined the amino acid substitutions of four variants, relative to the parent enzyme *Gv*Abf. They were modeled by the I-Tasser homology modeling server and structurally assessed by PyMOL Molecular Graphics System.

2 | MATERIALS AND METHODS

2.1 | Materials

Fermentas Plasmid DNA Isolation Kit and PCR Amplification Kit were used for *Gv*Abf active variants library construction (Fermentas-Life Science Technologies, Lithuania). All other chemicals including *p*NP-α-L-arabinofuranoside were obtained from Sigma Chemical (St. Louis, MO, USA).

2.2 | Bacterial strains, vectors, and growth conditions

Previously, six constructed *Escherichia coli* BL21 (λDE3) expression hosts carrying recombinant active alpha-L-arabinofuranosidase (*Gv*Abf) gene variants obtained from one-round error-prone PCR[24] were used as sources of *Gv*Abf enzyme variants. These strains, which also carried chaperon plasmid pG-Tf2 to increase the soluble *Gv*Abf protein variants,[24] were grown in Luria–Bertani broth (LB) media at 37°C and 225 rpm for overexpression of the genes. LB including 1% peptone, 0.5% yeast extract, and 0.5% NaCl was used for bacterial growth, supplementing kanamycin (50 μg/ml) and chloramphenicol (20 μg/ml). 1 mM isopropyl β-d-1-thiogalactopyranoside (IPTG) and 10 ng/ml tetracycline were used to overexpress *Gv*Abf variants and chaperon protein, respectively.

2.3 | The preparation of soluble protein extracts of *Gv*Abf active variants

The active *Gv*Abf variants (*Gv*Abf51, *Gv*Abf52, *Gv*Abf53, *Gv*Abf63, L307S, and Q90H/L307S) from a previously obtained library of 73 variants constructed by one-round error-prone PCR (epPCR) were used in this study. This library has been constructed as explained in Sürmeli et al. (2019).[24] Briefly, epPCR was performed to obtain the mutant library using the forward primer (5′-ggaacttgcatatggctacaaaaaaagcaacc-3′) and reverse primer (5′-ggaacatgaagcttttatcgttttcctaaacg-3′) in the following mutagenic conditions: 10× mutagenic PCR buffer, 10× mutagenic dNTP mix (5 mM dTTP, 5 mM CTTP, 2 mM dGTP, and 2 mM dATP) and 50 μM $MnCl_2$. Mutagenic PCR was applied as 30 cycles of denaturation at 95°C for 30 s, annealing at 55.9°C for 45 s, extension at 72°C for 90 s, as well as initial denaturation at 95°C for 3 min, and a final extension at 72°C for 10 min. PCR products were digested using *Nde*I and *Hin*dIII restriction enzymes, cloned into pET28a(+) expression vector and transformed to *E. coli* BL21 (λDE) with pG-Tf2. Then, soluble protein extracts of each active *Gv*Abf variant were obtained following procedure: Overnight cultures of *E. coli* BL21 (λDE3) strains were inoculated into 10 ml LB broth with 50 μg/ml kanamycin, 20 μg/ml chloramphenicol, and 10 ng/ml tetracycline, and grown at 37°C and 200 rpm. 1 mM IPTG was supplemented to each culture at OD_{600} of 0.7, and they were further grown at 37°C and 225 rpm for 4 h. The cultures were harvested at 4°C and 4500 *g* for 20 min by centrifugation. The pellets were dissolved in breaking buffer.[27] The cells were degraded by sonication on ice for 5 min (Sonopuls Ultrasonic Homogenizers, HD 2070; Bandelin, Berlin/Germany). The lysates were then harvested at 4°C and 12,000 *g* for 20 min and the supernatants (soluble protein extracts) were stored at −20°C as a source of the *Gv*Abf variants. The soluble protein extracts of the variants were screened to check their activity in the presence of 2 mM *p*NP-α-L-arabinofuranoside (*p*NPA) substrate (5 μl), sodium-acetate buffer (pH 5.0) (85 μl) and protein extract (10 μl) within a 96-well plate at 70°C for 10 min. Then, the OD_{420} of the mixtures was spectrophotometrically measured. The active variants from the library were analyzed at the biochemical, sequence, and structural levels.

2.4 | Biochemical analysis of *Gv*Abf variants

2.4.1 | Standard activity assay

The standard activity assay of the *Gv*Abf active variants was carried out supplementing 5 μl of *p*NP-α-L-arabinofuranoside (*p*NPA) substrate (2 mM), 85 μl of sodium-acetate (pH 5) buffer, and 10 μl soluble protein extract in a 96-well plate. This reaction mixture was incubated at 70°C and pH 5 for 10 min, and the reaction was then ended by adding the 100 μl Na_2CO_3 (1 M). The samples were spectrophotometrically measured at OD_{420}.

2.4.2 | Thermal stability

The temperature stability of the *Gv*Abf active variants and the parent enzyme were investigated at 71°C and pH 5 for 1 h. For this purpose, each soluble protein extract was incubated at 71°C and pH 5 over 1 h and then on ice for 5 min. The residual activity of each sample was determined by using the standard activity assay.

2.5 | Monitoring and sequencing of *Gv*Abf gene variants

Four *Gv*Abf gene variants and the parent *Gv*Abf gene were displayed using agarose gel electrophoresis. For this purpose, plasmid DNA isolation from the overnight cultures of *E. coli* BL21 (λDE3) including each *Gv*Abf variant was performed using plasmid DNA miniprep (Fermentas) according to the manufacturer's instructions, and the plasmid DNA concentrations were checked at 260 nm by Nanodrop ND1000. PCR was applied as mentioned above and the PCR products were checked in agarose gel electrophoresis (1%).

The genes of *Gv*Abf and its variants were sequenced by the dideoxynucleotide chain termination technique using 16 and 80 capillary, 3130XL (Applied Biosystem, CA, USA).[28] Finch TV (version 1.4.0) was utilized for the analysis of nucleotide chromatograms of the genes. Furthermore, the amino acid sequence differences between the *Gv*Abf variants and the parent enzyme were analyzed by Clustal Omega.[29]

2.6 | Homology modeling and structural analysis

The three-dimensional homology model of the parent enzyme *Gv*Abf was built using homology modeling by I-Tasser online server.[30–32] Also, the model was analyzed using PyMOL Molecular Graphics System, Version 2.0 (Schrödinger, LLC). Amino acid sequences of *Gv*Abf and templates used in homology modeling were aligned by Clustal Omega.[29]

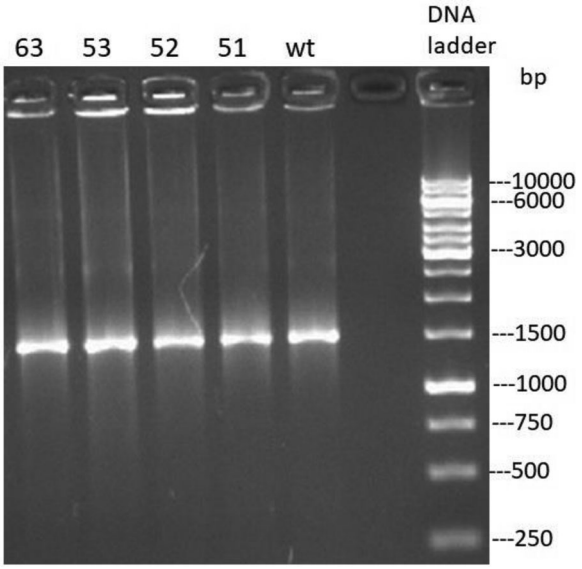

FIGURE 1 Agarose gel (1%) image of the gene of *Gv*Abf (wt) and its four active variants (*Gv*Abf51, *Gv*Abf52, *Gv*Abf53, and *Gv*Abf63)

2.7 | Data presentation and statistical analysis

Ordinary one-way ANOVA was implemented to statistically analyze by GraphPad Prism version 6.00 for Windows (GraphPad Software, La Jolla, CA, USA). All experiments were carried out in triplicate.

3 | RESULTS AND DISCUSSION

In this study, *Gv*Abf active variants obtained by directed evolution were investigated at biochemical, sequence, and structural levels, relative to the parent enzyme (*Gv*Abf). The PCR products of *Gv*Abf gene variants were analyzed by agarose gel electrophoresis. Each band of the genes was located at near 1500 bp band size, confirming that every construct possessed a single *Gv*Abf gene variant (Figure 1). Two previous works also demonstrated that the *Gv*Abf gene is 1509 bp in length.[18,24] The genes of four active variants and two previously characterized variants (L307S and Q90H/L307S)[24] were overexpressed in *E. coli* BL21 (λDE3) cultures induced by IPTG to obtain the soluble protein extracts including each variant and *Gv*Abf. Biochemical analyses were performed on soluble protein extracts including the *Gv*Abf and six variants (*Gv*Abf51, *Gv*Abf52, *Gv*Abf53, *Gv*Abf63, L307S, and Q90H/L307S).

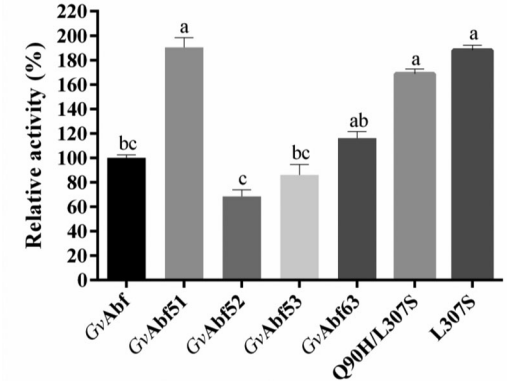

FIGURE 2 Relative activity of *Gv*Abf and its six active variants at 70°C and pH 5.0 using *p*NPA substrate. Different letters ($^{a-c}$) indicate significant statistical differences among the average values of variants ($p < 0.05$, Tukey's test) (Table S1).

3.1 | Biochemical analysis of *Gv*Abf and its variants

3.1.1 | Activity determination

The activity of six active *Gv*Abf variants and *Gv*Abf was determined at 70°C and pH 5.0 using *p*NPA substrate. The results showed that the variants *Gv*Abf51 and L307S had the highest activity among other variants and they exhibited as much about two-fold activity as relative to *Gv*Abf. In addition, Q90H/L307S variant possessed high activity of approximately 70%, relative to the *Gv*Abf and there was not any significant difference between activities of Q90H/L307S and two variants (*Gv*Abf51 and L307S). In previous work, the L307S and Q90H/L307S variants possessed higher specific activity, relative to *Gv*Abf.[24] Also, the activity of the *Gv*Abf63 variant was 20% more than the parent enzyme, and it was lower than *Gv*Abf51, L307S, and Q90H/L307S. Also, the *Gv*Abf52 variant had 40% less activity, compared to the parent enzyme (Figure 2 and Table S1). These differences in activity indicated that there may be significant mutational differences among variants.

3.1.2 | Determination of thermal stability of *Gv*Abf variants

Thermal stability of *Gv*Abf and six variants was determined at 71°C and pH 5 for 1 h using *p*NPA substrate. The results showed that the *Gv*Abf52 had the highest thermal stability, with remaining 80% of residual activity upon incubation of 1 h. This residual activity was about 2.5 times greater compared to the parent enzyme showing about 30% residual

TABLE 1 Six active *Gv*Abf variants and their amino acid substitutions

*Gv*Abf variant	Amino acid substitution	Reference
*Gv*Abf51	L307S	This study
*Gv*Abf52	S215N, L307S, H473P, G476C	This study
*Gv*Abf53	A255D, Y257H, L307S	This study
*Gv*Abf63	H30D, Q90H, L307S	This study
L307S	L307S	24
Q90H/L307S	Q90H, L307S	24

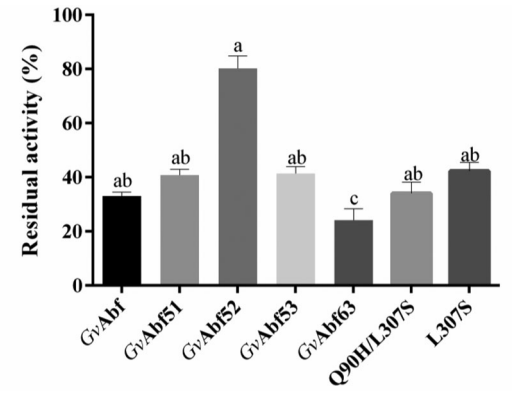

FIGURE 3 Thermostability analysis of six *Gv*Abf active variants at 70°C and pH 5.0 upon incubation of 1 h, compared to the parent enzyme. Different letters ($^{a-c}$) indicate significant statistical differences among the average values of variants ($p < 0.05$, Tukey's test) (Table S1).

activity. On the other hand, the lowest thermal stability belonged to *Gv*Abf63 exhibiting 24.1% of residual activity. The residual activity values of the other four variants (*Gv*Abf51, *Gv*Abf53, L307S, and Q90H/L307S) were not statistically significant, compared to the wild-type enzyme (Figure 3 and Table S2).

3.2 | Comparative sequence and structural analyses of *Gv*Abf enzyme variants

3.2.1 | Comparative sequence analysis

The nucleotide sequences of *Gv*Abf gene variants and the parent gene were determined by Sanger dideoxynucleotide chain termination (Supporting Information) and then converted into amino acid sequences as summarized in Table 1. According to these results, *Gv*Abf51 possessed only one amino acid substitution as L307S, and *Gv*Abf52 had four amino acid substitutions (S215N, L307S, H473P, and G476C). In addition, *Gv*Abf53 (A255D, Y257H, L307S) and *Gv*Abf63 (H30D, Q90H, L307S) were found as triple mutants. Interestingly, all variants conserved the L307S replacement. The previous study showed that the L307S variant enhanced the specific activity of α-L-arabinofuranosidase on *p*NPA by 2.5-fold, compared to the parent enzyme, suggesting that this amino acid replacement may act a key role in *Gv*Abf activity.[24] In this study, the activity analyses supported the result in which *Gv*Abf51 had significantly higher activity than the parent enzyme and other variants, similar to the L307S variant (Figure 2). On the other hand, the other amino acid substitutions in *Gv*Abf52, *Gv*Abf53, and *Gv*Abf63 somehow might have suppressed the beneficial effect of L307S on the enzyme activity (Table 1).

3.2.2 | Comparative structural analysis of *Gv*Abf enzyme variants

The template three-dimensional structures having the highest statistical significance of PDB library were identified by LOMETS, a meta-server threading program, and for this purpose, many templates of glycoside hydrolase 51 (GH51) family proteins were utilized to align with the α-L-arabinofuranosidase. Thus, two PDB hits were detected by the LOMETS: 1QW9 of *Geobacillus stearothermophilus* T-6,[33] and 2C8N of *Clostridium thermocellum*.[34] Amino acid sequence alignment analysis was performed by Clustal Omega.[29] According to this analysis, 1QW9 had 98.41% of amino acid sequence identity with the *Gv*Abf (Figure 4A). This identity was higher than that of 2C8N (68.66%) (Supporting Information). In addition, the alignment of the three-dimensional structure showed that *Gv*Abf and 1QW9 were highly similar and compatible with each other in terms of entire folding patterns (Figure 4B).

A previous study has reported a description of 1QW9 crystal structures with high resolution, which is a member of the GH51 family. It is a hexameric enzyme and each monomer is composed of two domains called a $(\beta/\alpha)_8$-barrel and a 12-stranded β sandwich with jelly-roll topology.[33] TIM barrel domain, which consists of residues 20–383, is bound to catalytic activity in many GH families including GH51[35] including the catalytic residues (E29, E175, and E294) of the GH51

FIGURE 4 Alignment of *Gv*Abf (violet) and 1QW9 (green) at the sequence (A) and structural level (B). The three-dimensional homology model was built by I-Tasser online server and analyzed using PyMOL Molecular Graphics System, Version 2.0 (Schrödinger, LLC).

alpha-L-arabinofuranosidase.[36–38] In the present study, it was shown that some amino acid substitutions of different variants were located in the TIM barrel domain: L307S in *Gv*Abf51, S215N/L307S in *Gv*Abf52, A255D/Y257H/L307S in *Gv*Abf53, and H30D/Q90H/L307S in *Gv*Abf63.

L307S was kept in all variants and this residue was located in one α-helix, adjacent to a loop connecting to β-strand with E294 (Figure 5A), which is nucleophile residue.[36] Sürmeli et al. (2019) have shown that L307S led to a significant increase of specific activity of *Gv*Abf.[24] We confirmed that two different (*Gv*Abf51 and L307S) variants having only L307S substitution had significantly higher relative activity than that of the parent enzyme *Gv*Abf (Figure 2). Thus, we suggested that L307S substitution may result in stronger interaction between E294 and the substrate, thereby enhancing catalytic action. Also, the proximity of S215 to E175 in *Gv*Abf was noteworthy (Figure 5B). E175 is an acid–base residue that directly plays a role in substrate catalysis.[37] In the present study, the *Gv*Abf52 variant including S215N substitution had the lowest activity (Figure 2). This indicated that the S215N substitution may weaken the interaction of amino acid E175 with the substrate. The same *Gv*Abf52 variant also had the highest thermostability, compared to the parent

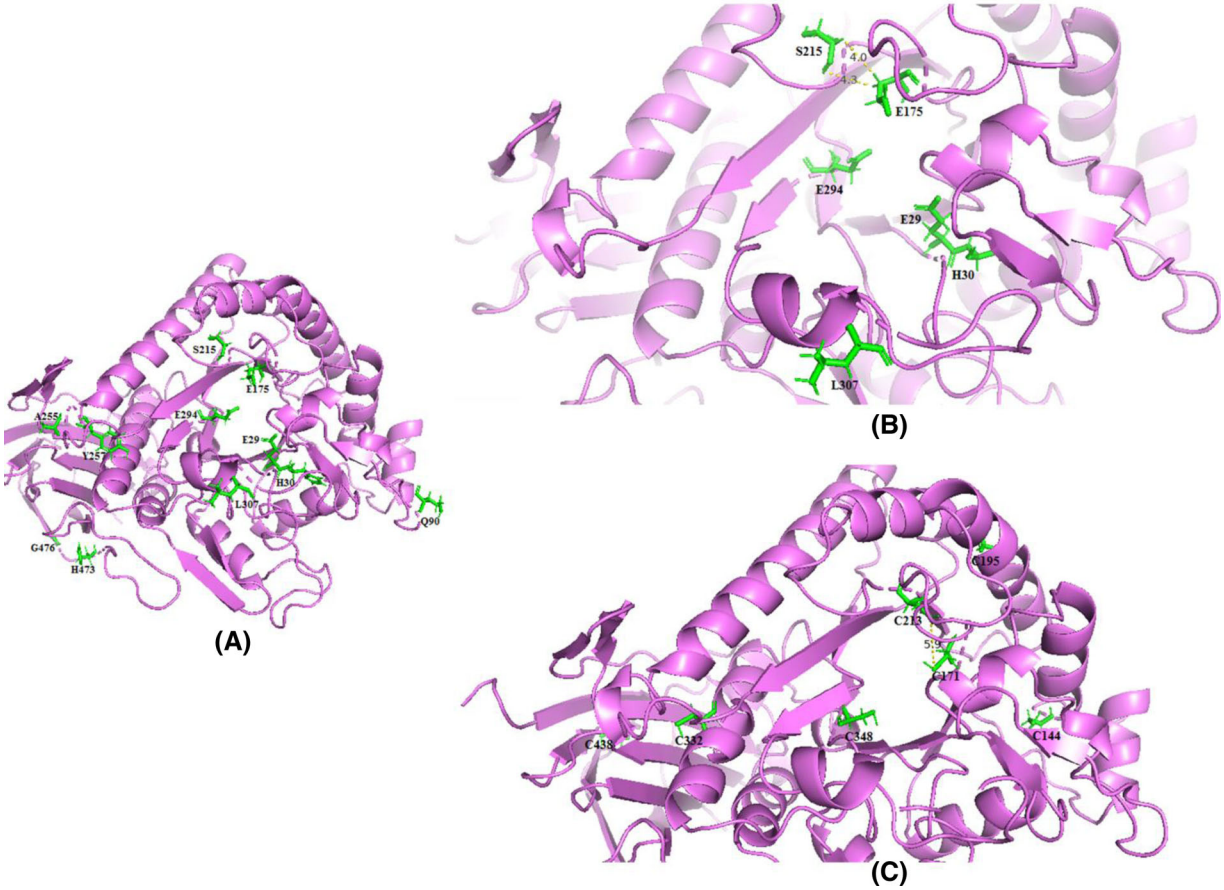

FIGURE 5 Cartoon image of *Gv*Abf model with three catalytic residues (E29, E275, and E294) and the replaced residues in four *Gv*Abf variants (H30, Q90, S215, A255, Y257, L307, H473, and G476) (A). Key residues affecting catalytic activity of *Gv*Abf (B). Cysteine residues are found in *Gv*Abf and potential residues that can form a disulfide bond (C). The residues were displayed as stick representations. The three-dimensional homology model was built by I-Tasser online server and analyzed using PyMOL Molecular Graphics System, Version 2.0 (Schrödinger, LLC).

enzyme (Figure 3). This may be explained that S215N, L307S, H473P, and G476C together may improve overall structure rigidity by forming a disulfide (C–C) bond between C171 and C213, becoming a closer location to each other (Figure 5C). The *Gv*Abf63 variant, which has higher activity than the parent enzyme, but significantly lower activity than *Gv*Abf51 with L307S displacement, possessed H30D, Q90H, and L307S substitutions (Table 1). Our previous study has shown that the specific activity of the pure Q90H/L307S double mutant was similar to that of the pure L307S single mutant.[24] Here, we confirmed that relative activities of Q90H/L307S and L307S were similar to each other. We could conclude that the Q90H displacement may not have a role in the enzyme activity. A decrease in the activity of *Gv*Abf63 relative to *Gv*Abf51 can be attributed to the H30D amino acid displacement. H30 residue was covalently bound to E29 (Figure 5B), which is proposed as a third catalytic residue of 1QW9.[33,38] This substitution may partly suppress the beneficial effect of L307S on the activity of the *Gv*Abf63 variant and may lead to the steric hindrance of E29 catalytic residue.

4 | CONCLUSION

We identified key residues affecting activity and thermostability in four active variants (*Gv*Abf51, *Gv*Abf52, *Gv*Abf53, and *Gv*Abf63) obtained by directed enzyme evolution. L307S amino acid substitution was the common displacement among all variants and increased the activity by two-fold in *Gv*Abf51, relative to the parent *Gv*Abf enzyme. L307 residue was located on an α-helix separated by a loop from the β-sheet carrying the catalytic nucleophile E294. Thus, we suggested that this residue may be critical for *Gv*Abf enzyme activity. Also, another key residue on *Gv*Abf activity was determined as H30, which was covalently bound to E29 third catalytic residue. *Gv*Abf63 variant including H30D possessed lower activity

than that of *Gv*Abf51 variant with L307S amino acid substitution. We proposed that H30D amino acid substitution may partly disrupt the activity of the *Gv*Abf63 variant and decrease the beneficial influence of L307S substitution on its activity by sterically hindering E29. We identified that S215 may also be an important residue affecting the activity of *Gv*Abf. Regarding this, *Gv*Abf52 including S215N had very low activity, compared to the parent enzyme and the other variants. S215N substitution was highly close to E175, which is acid–base residue and directly involved in substrate catalysis. We proposed that S215N substitution may severely decrease the *Gv*Abf52 activity, thereby weakening the interaction between E175 and the substrate. Also, we determined that *Gv*Abf52 possessed the highest thermal stability, relative to the parent enzyme and the other variants. We could explain this phenomenon that S215N, L307S, H473P, and G476C substitutions may synergistically increase the thermostability of *Gv*Abf52 by becoming a closer location of C171 and C213 to form a disulfide (C–C) bond. Taken together, this study demonstrated that directed enzyme evolution was a powerful approach to determine the key amino acid residues underlying *Gv*Abf characteristics.

ACKNOWLEDGMENT

The authors would like to thank Biotechnology and Bioengineering Research Center at İzmir Institute of Technology for the facilities and technical support.

CONFLICT OF INTEREST

The authors declare that there is no conflict of interest.

REFERENCES

1. Taiz L, Zeiger E. Plant physiology. 3rd ed. Sunderland, Massachusetts USA: Sinauer Associates Inc.; 2010.
2. Wood TM, McCrae SI, Bhat KM. The mechanism of fungal cellulase action. Synergism between enzyme components of *Penicillium pinophilum* cellulase in solubilizing hydrogen bond-ordered cellulose. Biochem J. 1989;260(1):37–43.
3. Sánchez OJ, Cardona CA. Trends in biotechnological production of fuel ethanol from different feedstocks. Bioresour Technol. 2008;99(13):5270–95.
4. Kaji A. Dexter French 1918–1981. Adv Carbohydr Chem Biochem. 1984;42:383–94.
5. Hoffmam ZB, Oliveira LC, Cota J, Alvarez TM, Diogo JA, de Oliveira Neto M, et al. Characterization of a hexameric exo-acting GH51 α-l-arabinofuranosidase from the mesophilic Bacillus subtilis. Mol Biotechnol. 2013;55(3):260–7.
6. Numan M, Bhosle N. Alpha-L-arabinofuranosidases: the potential applications in biotechnology. J Ind Microbiol Biotechnol. 2006;33(4):247–60.
7. Aryan A-P, Wilson B, Strauss C-R, Williams P-J. The properties of glycosidases of Vitis vinifera and a comparison of their beta-glycosidase activity with that of exogenous enzymes. An assessment of possible applications in enology. Am J Enol Vitic. 1987;38:182–8.
8. Saha B. Alpha-L-arabinofuranosidases: biochemistry, molecular biology and application in biotechnology. Biotechnol Adv. 2000;18(5):403–23.
9. Gao D, Uppugundla N, Chundawat SPS, Yu X, Hermanson S, Gowda K, et al. Hemicellulases and auxiliary enzymes for improved conversion of lignocellulosic biomass to monosaccharides. Biotechnol Biofuels. 2011;4:5.
10. Raweesri P, Riangrungrojana P, Pinphanichakarn P. Alpha-L-arabinofuranosidase from *Streptomyces* sp. PC22: purification, characterization and its synergistic action with xylanolytic enzymes in the degradation of xylan and agricultural residues. Bioresour Technol. 2008;99(18):8981–6.
11. Lee RC, Hrmova M, Burton RA, Lahnstein J, Fincher GB. Bifunctional family 3 glycoside hydrolases from barley with alpha-L-arabinofuranosidase and beta-D-xylosidase activity. Characterization, primary structures, and COOH-terminal processing. J Biol Chem. 2003;278(7):5377–87.
12. Rahman AK, Kato K, Kawai S, Takamizawa K. Substrate specificity of the alpha-L-arabinofuranosidase from *Rhizomucor pusillus* HHT-1. Carbohydr Res. 2003;338(14):1469–76.
13. Debeche T, Cummings N, Connerton I, Debeire P, O'Donohue MJ. Genetic and biochemical characterization of a highly thermostable alpha-L-arabinofuranosidase from *Thermobacillus xylanilyticus*. Appl Environ Microbiol. 2000;66(4):1734–6.
14. Canakci S, Kacagan M, Inan K, Belduz AO, Saha BC. Cloning, purification, and characterization of a thermostable alpha-L-arabinofuranosidase from *Anoxybacillus kestanbolensis* AC26Sari. Appl Microbiol Biotechnol. 2008;81(1):61–8.
15. Morozkina EV, Slutskaya ES, Fedorova TV, Tugay TI, Golubeva LI, Koroleva OV. [Extremophilic microorganisms: biochemical adaptation and biotechnological application (review)]. Appl Biochem Microbiol. 2010;46:5–20.
16. Geng A, Wu J, Xie R, Wang H, Wu Y, Li X, et al. Highly thermostable GH_{51} α-arabinofuranosidase from *Hungateiclostridium clariflavum* DSM 19732. Appl Microbiol Biotechnol. 2019;103:3783–93.
17. Tu T, Li X, Meng K, Bai Y, Wang Y, Wang Z, et al. A GH_{51} α-L-arabinofuranosidase from *Talaromyces leycettanus* strain JCM12802 that selectively drives synergistic lignocellulose hydrolysis. Microb Cell Fact. 2019;18(1):138.
18. İlgü H, Sürmeli Y, Şanlı-Mohamed G. Effects of selected lactobacilli on the functional properties and stability of gluten-free sourdough bread. Eur Food Res Technol. 2018;244:1627–36.
19. Lee SH, Lee YE. Cloning, expression, and characterization of a thermostable GH_{51} α-L-arabinofuranosidase from Paenibacillus sp. DG-22. J Microbiol Biotechnol. 2014;24(2):236–44.
20. Canakci S, Belduz AO, Saha BC, Yasar A, Ayaz FA, Yayli N. Purification and characterization of a highly thermostable alpha-L-arabinofuranosidase from *Geobacillus caldoxylolyticus* TK_4. Appl Microbiol Biotechnol. 2007;75(4):813–20.
21. Kaur J, Sharma R. Directed evolution: an approach to engineer enzymes. Crit Rev Biotechnol. 2006;26(3):165–99.
22. Cobb RE, Chao R, Zhao H. Directed evolution: past, present, and future. AIChE J. 2013;59(5):1432–40.
23. Bloom JD, Arnold FH. In the light of directed evolution: pathways of adaptive protein evolution. Proc Natl Acad Sci. 2009;106(Suppl 1):9995–10000.

24. Sürmeli Y, İlgü H, Şanlı-Mohamed G. Improved activity of α-L-arabinofuranosidase from *Geobacillus vulcani* GS90 by directed evolution: investigation on thermal and alkaline stability. Biotechnol Appl Biochem. 2019;66(1):101–7.
25. Arab-Jaziri F, Bissaro B, Tellier C, Dion M, Fauré R, O'Donohue MJ. Enhancing the chemoenzymatic synthesis of arabinosylated xylo-oligosaccharides by GH51 α-L-arabinofuranosidase. Carbohydr Res. 2015;401:64–72.
26. Giacobbe S, Vincent F, Faraco V. Development of an improved variant of GH51 α-l-arabinofuranosidase from *Pleurotus ostreatus* by directed evolution. N Biotechnol. 2014;31(3):230–6.
27. Stephens DE, Singh S, Permaul K. Error-prone PCR of a fungal xylanase for improvement of its alkaline and thermal stability. FEMS Microbiol Lett. 2009;293(1):42–7.
28. Sanger F, Nicklen S, Coulson AR. DNA sequencing with chain-terminating inhibitors. Proc Natl Acad Sci U S A. 1977;74(12):5463–7.
29. Madeira F, Park YM, Lee J, Buso N, Gur T, Madhusoodanan N, et al. The EMBL-EBI search and sequence analysis tools APIs in 2019. Nucleic Acids Res. 2019;47(W1):W636–41.
30. Roy A, Kucukural A, Zhang Y. I-TASSER: a unified platform for automated protein structure and function prediction. Nat Protoc. 2010;5:725–38.
31. Yang J, Yan R, Roy A, Xu D, Poisson J, Zhang Y. The I-TASSER Suite: protein structure and function prediction. Nat Methods. 2015;12:7–8.
32. Yang J, Zhang Y. I-TASSER server: new development for protein structure and function predictions. Nucleic Acids Res. 2015;43:W174–81.
33. Hövel K, Shallom D, Niefind K, Belakhov V, Shoham G, Baasov T, et al. Crystal structure and snapshots along the reaction pathway of a family 51 alpha-L-arabinofuranosidase. EMBO J. 2003;22(19):4922–32.
34. Taylor EJ, Smith NL, Turkenburg JP, D'Souza S, Gilbert HJ, Davies GJ. Structural insight into the ligand specificity of a thermostable family 51 arabinofuranosidase, Ara f 51, from *Clostridium thermocellum*. Biochem J. 2006;395(1):31–7.
35. Kamitori S, Kondo S, Okuyama K, Yokota T, Shimura Y, Tonozuka T, et al. Crystal structure of *Thermoactinomyces vulgaris* R-47 alpha-amylase II (TVAII) hydrolyzing cyclodextrins and pullulan at 2.6 A resolution. J Mol Biol. 1999;287(5):907–21.
36. Shallom D, Belakhov V, Solomon D, Shoham G, Baasov T, Shoham Y. Detailed kinetic analysis and identification of the nucleophile in alpha-L-arabinofuranosidase from *Geobacillus stearothermophilus* T-6, a family 51 glycoside hydrolase. J Biol Chem. 2002;277(46):43667–73.
37. Shallom D, Belakhov V, Solomon D, Gilead-Gropper S, Baasov T, Shoham G, et al. The identification of the acid-base catalyst of alpha-arabinofuranosidase from *Geobacillus stearothermophilus* T-6, a family 51 glycoside hydrolase. FEBS Lett. 2002;514(2-3):163–7.
38. Debeche T, Bliard C, Debeire P, O'Donohue MJ. Probing the catalytically essential residues of the alpha-L-arabinofuranosidase from *Thermobacillus xylanilyticus*. Protein Eng. 2002;15(1):21–8.

SUPPORTING INFORMATION

Additional supporting information can be found online in the Supporting Information section at the end of this article.

How to cite this article: Sürmeli Y, Şanlı-Mohamed G. Structural and functional analyses of GH51 alpha-L-arabinofuranosidase of *Geobacillus vulcani* GS90 reveal crucial residues for catalytic activity and thermostability. Biotechnol Appl Biochem. 2022;1–9.
https://doi.org/10.1002/bab.2423